

# Facile Fabrication of Anisotropic Multicompartmental Microfibers Using Charge Reversal Electrohydrodynamic Co-Jetting

Jaeyu Lee, Seongjun Moon, Yong Bin Han, SeungJae Yang,\* Joerg Lahann,\* and Kyung Jin Lee\*

Anisotropic microstructures are utilized in various fields owing to their unique properties, such as reversible shape transitions or on-demand and sequential release of drug combinations. In this study, anisotropic multicompartmental microfibers composed of different polymers are prepared via charge reversal electrohydrodynamic (EHD) co-jetting. The combination of various polymers, such as thermoplastic polyurethane, poly(D,L-lactide-co-glycolide), poly(vinyl cinnamate), and poly(methyl methacrylate), results in microfibers with distinct compositional boundaries. Charge reversal during EHD co-jetting enables facile fabrication of multicompartmental microfibers with the desired composition and tunable inner architecture, broadening their spectrum of potential applications, such as functional microfibers and cell scaffolds with multiple physical and chemical properties.

applications, such as spatio-selective cell scaffolds,<sup>[1,2]</sup> drug carriers with selective or controlled release functions,<sup>[3,4]</sup> and colloidal self-assembly.<sup>[5,6]</sup> Macroscopically, two major types of anisotropies, 1) surface anisotropy and 2) bulk anisotropy, have been continuously reported so far.<sup>[7]</sup> For surface anisotropy, surface patchy methods, including pickering emulsions,<sup>[8,9]</sup> and sputtering methods, have been utilized.<sup>[10,11]</sup> However, for applications that require both surface and bulk anisotropy, micro-building blocks comprising several different materials with distinct compartments are required. Several approaches have been reported, such as particle replication in non-wetting template methods,<sup>[12–14]</sup>

microfluidic methods,<sup>[15,16]</sup> and phase-separation using block copolymers.<sup>[17]</sup> Our series of studies on the preparation of multicompartmental microparticles and non-particle shapes, such as fibers, cylinders, and disks using electrohydrodynamic (EHD) co-jetting can be another promising alternative to achieve this goal.<sup>[18–20]</sup>

EHD co-jetting involves the acceleration of two or more polymeric solutions in an electrical field that are delivered under a laminar flow regimen.<sup>[21–24]</sup> Various structures with distinct compartments, such as microdisks, microparticles, microfibers, and microcylinders, can be prepared by modified electrospraying and EHD co-jetting, followed by sectioning microfiber bundles.<sup>[25,26]</sup> However, it is still challenging to introduce materials with vastly distinct properties into a single micro-building block because their EHD properties can significantly delineate if a high electrical potential is applied. So far, most studies on EHD co-jetting have involved chemically or physically similar polymeric solutions. Examples include the introduction of poly(D,L-lactide-co-glycolide) (PLGA) in one compartment, and alkyne-PLGA or a mixture of PLGA and other polymers in the other compartment to prepare Janus-type microparticles or fibers.<sup>[27,28]</sup> Another example is Janus core/shell jetting.<sup>[29]</sup> As the overall jetting behavior is governed by the shell solution, different materials can be introduced into each core, and after shell removal, Janus-type microfibers and cylinders composed of completely different materials can be obtained. To optimize EHD co-jetting conditions, the properties of different polymeric solutions, including viscosity, concentration, surface tension, conductivity, and dielectric constant, need to be sequentially adjusted, which can be a tedious

## 1. Introduction

Significant attention has been paid to the preparation of anisotropic micro-building blocks owing to their promising

J. Lee, K. J. Lee  
 Department of Chemical Engineering and Applied Chemistry  
 College of Engineering  
 Chungnam National University  
 99 Daehak-ro (st), Yuseong-gu, Daejeon 34134, Republic of Korea  
 E-mail: kjlee@cnu.ac.kr

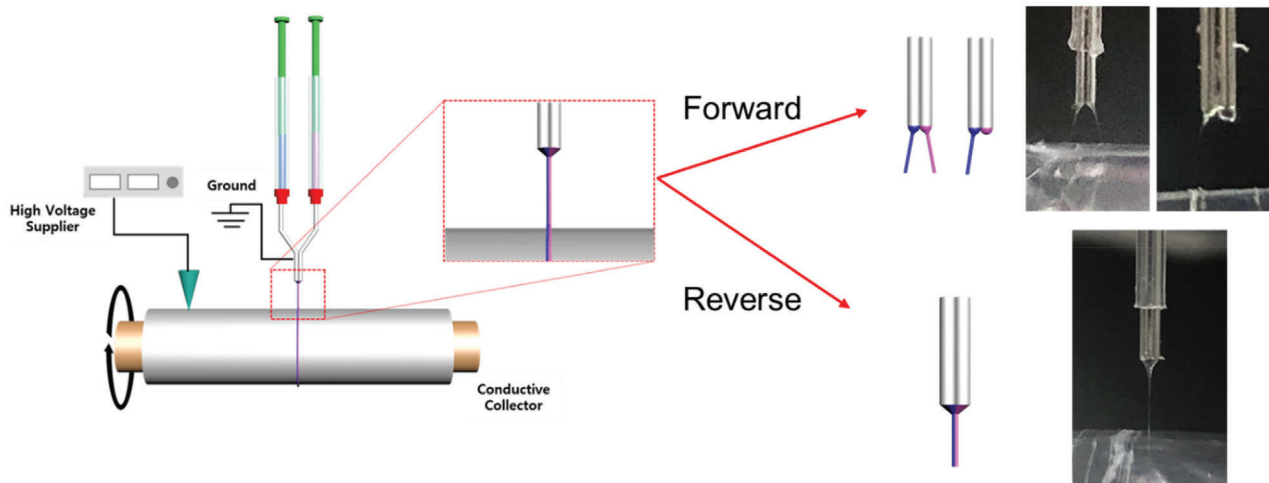
S. Moon  
 Information and Electronics Research Institute  
 Korea Advanced Institute of Science and Technology (KAIST)  
 291 Daehak-ro (st), Yuseong-gu, Daejeon 34141, Republic of Korea

Y. B. Han, S. J. Yang  
 Advanced Nanohybrids Laboratory  
 Department of Chemistry and Chemical Engineering  
 Education and Research Center for Smart Energy and Materials  
 Inha University  
 Incheon 22212, Republic of Korea  
 E-mail: sjyang@inha.ac.kr

J. Lahann  
 Department of Chemical Engineering  
 University of Michigan  
 Ann Arbor, MI 48109, USA  
 E-mail: lahann@umich.edu

 The ORCID identification number(s) for the author(s) of this article can be found under <https://doi.org/10.1002/marc.202100560>

DOI: 10.1002/marc.202100560



**Scheme 1.** Schematic of conventional jetting (forward) and charge reversal jetting (reverse) and digital photographs of biphasic microfiber fabrication.

optimization task in practice.<sup>[30,31]</sup> Therefore, simple and versatile methods are required to prepare compartmentalized microfibers with various types of polymers. Recently, we reported the charge reversal electro-jet writing (CREW) method to fabricate several micrometer-thick polymeric threads for jet-writing.<sup>[32]</sup> The most important feature of the CREW method is that the electrical potential is applied to the collector (not needle) for jet formation, in contrast to the previous reports that adopted conventional jetting setup (applying voltage on needle). This method enables EHD co-jetting with two or more different polymeric solutions without a tedious optimization process.

Herein, we report a versatile approach for preparing microfibers with distinct compartments using the charge reversal EHD co-jetting method. The inverse configuration of EHD co-jetting, with a positive voltage on the collector and ground electrode on needles, is beneficial not only for generating polymeric threads without whipping motion but also for the simultaneous jetting of different polymeric solutions by suppressing the EHDs. Janus and even triphasic-type microfibers with diameters of a few microns were prepared using various combinations of polymer, such as thermoplastic polyurethane (TPU), PLGA, poly(methyl methacrylate) (PMMA), and poly(vinyl cinnamate) (PVCi).

## 2. Results and Discussions

The overall procedure of charge reversal jetting for multicompartmental microfibers is schematically illustrated in **Scheme 1**. In contrast to conventional jetting, the ground electrode is connected to the needles that deliver the polymeric solutions. A positive voltage ( $\approx 3.0\text{--}5.0$  kV) is applied to the rotating collector, usually rotating at a speed of 20 rpm. The level of applied voltage of reverse jetting is much lower than that of forward jetting (12–15 kV) to obtain same jet-behavior. This is one of the greatest advantages for reverse jetting in terms of energy saving, which is important issue in electrospinning science.<sup>[33]</sup> The tip-to-collector distance is typically 5–10 mm. This charge reversal setup has several advantages as reported previously.<sup>[34–36]</sup> How-

ever, one important advantage is the suppression of EHDs during jetting by reducing the accumulation of extra charges on the solution.<sup>[32]</sup> As illustrated in **Scheme 1**, simultaneous jetting of two different polymeric solutions generally results in a separated jet or single jet (conventional setup, forward system). However, it is possible to perform co-jetting of two different polymeric solutions in a charge reversal system.

**Figure 1a** shows a photograph taken during charge reversal EHD co-jetting of PLGA and TPU solutions. The whipping motion of the jet thread was completely suppressed, allowing the microfiber bundle to be obtained using a simple rotating collector. As illustrated in the inset of **Figure 1a**, two different solutions formed a single Taylor cone under certain conditions (applied voltage: 3.0–5.0 kV, flow rate:  $150\ \mu\text{L h}^{-1}$ ) and maintained their laminar flow. The bicompartmental architecture was sufficiently distinguishable even in the field emission scanning electron microscopy (FE-SEM) image of microfiber bundles (**Figure 1b**), exhibiting clear boundaries and different surface morphologies on each surface. A stable jet thread without whipping motion makes it possible to obtain fiber bundles, which could be cryo-sectioned to prepare Janus-type microcylinders.<sup>[25]</sup> The results are microcylinders composed of completely different polymeric materials. Blue and green dyes were added to the TPU and PLGA solutions, respectively, for distinct visualization under confocal laser scanning microscopy (CLSM). A clear boundary between the two implied successful compartmentalization during jetting and sectioning (**Figure 1c**).

As aforementioned, the simultaneous jetting with different polymers is also possible using core/shell needle configuration.<sup>[18,26,29,37]</sup> However, this behavior is generally impossible to obtain using the conventional forward-jetting with side-by-side needle configuration, which provide several benefits such as easy preparation of needle structures and enabling multicompartmentalization over Janus manner (so far, three to seven compartments).<sup>[25]</sup> This charge reversal EHD co-jetting provides a powerful method to prepare multicompartmental microfibers with different type of materials using side-by-side needle configuration.

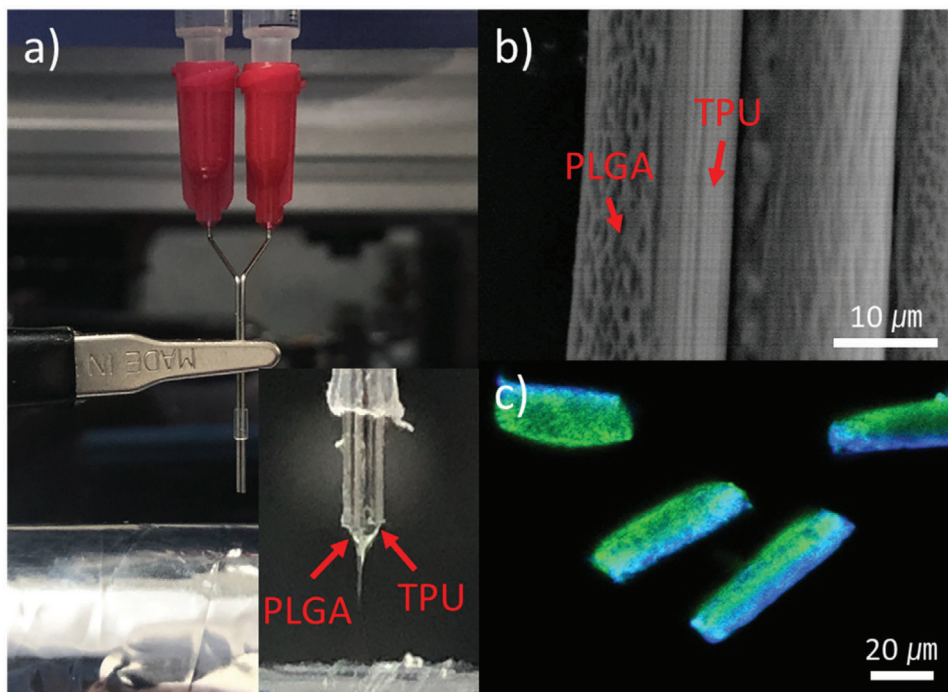


**Figure 1.** a) Photograph of fabrication process for microfiber with TPU and PLGA. b) FE-SEM and c) CLSM images of TPU and PLGA biphasic microstructures. TPU and PLGA are represented by blue and green colors, respectively.

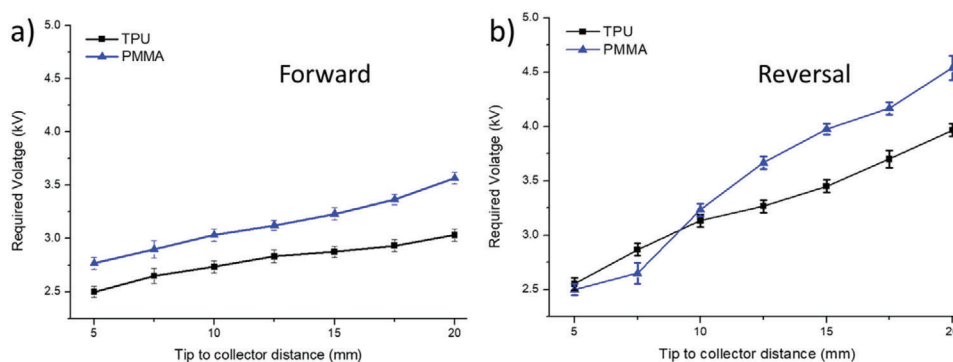


**Figure 2.** Required voltage to generate stable Taylor cone of TPU and PMMA solutions in a) a forward system and b) a reversal system as a function of tip-to-collector distance.

Apart from reducing the extra charges accumulated in the jet thread, the configuration also promotes the generation of a “co-Taylor cone,” which is the most important criterion for jet formation.<sup>[32,34]</sup> The formation of a stable Taylor cone after voltage application is crucial for jet launching. In the case of a forward system (applied voltage on the needle), the required voltage for Taylor cone formation depends on the type of polymeric solution. Although obtaining stable jetting conditions via a forward system is extremely difficult, it is easy to generate the Taylor cone itself. As illustrated in **Figure 2a**, the required voltages for Taylor cone formation of either TPU or PMMA single solution in the forward system are different, and these differences are independent of the tip-to-collector distance. Therefore, it is diffi-

cult to find common conditions for co-Taylor cone formation in a forward system. By contrast, in the reversal system, the required voltage for each Taylor cone largely depends on the tip-to-collector distance (**Figure 2b**). This is because the required voltage in the reversal system is related to the induced dipoles in the polymeric solution, which strongly depends on the tip-to-collector distance. In the forward system, the jetting behavior is governed by the solution conductivity, which is related to the intrinsic properties of the polymeric solution. The dipole moment of the polymeric solution depends on the dielectric constant of its components. In general, most polymers have similar dielectric constants,<sup>[38,39]</sup> and most solutions are composed of the same jetting solvent, resulting in similar dielectric constants for all polymeric solutions.

**Table 1.** Properties of polymer solutions.

Polymer	Solvent [THF/DMF, v/v]	Concentration [% w/v]	Conductivity [ $\mu\text{S cm}^{-1}$ ]
TPU	6/4	20	$0.57 \pm 0.05$
PLGA	6/4	70	$0.26 \pm 0.05$
PMMA	5/5	40	$1.47 \pm 0.05$
PVCi	6/4	70	$0.33 \pm 0.05$

However, the conductivity largely depends on the type of additives in the organic solutions,<sup>[40]</sup> resulting in large differences in the conductivity of various polymer solutions (see **Table 1**). Therefore, in a reversal system, optimization of conditions to generate co-Taylor cones of different polymeric solutions can be achieved by simply adjusting the tip-to-collector distance, whereas it is difficult to obtain co-jetting conditions in a forward system.

The reversal jetting configuration is quite versatile and can be applied to various combinations of polymers to create bicompartamental microfibers in a Janus manner. **Figure 3** shows the FE-SEM and CLSM images of microfiber bundles composed of a combination of two different polymers, such as TPU/PMMA (a,e), PLGA/PVCi (b,f), PLGA/PMMA (c,g; inset: CLSM image of microcylinders after sectioning), and PMMA/PVCi (d,h; **Figure 3h** shows cross-sectional CLSM image of fibers). As revealed by the FE-SEM images, microfiber bundles with a single fiber thickness of 10  $\mu\text{m}$  can be fabricated irrespective of the polymer type and combination. The identical thickness of each fiber implies that the fiber thickness is determined by the process parameters and not the material properties. Bicompartamental features with obvious boundaries can be observed in each FE-SEM image; however, it is difficult to identify each polymer. Here, the CLSM images are beneficial as the color emanating from photoluminescent dyes incorporated into each polymeric solution provides clear visual distinction. The clear boundaries of each compartment imply that laminar flow was well maintained, and no intermixing occurred during the process.

The type of polymer applicable in this system is not limited in TPU, PLGA, PMMA, and PVCi. Any polymer which is soluble in the THF/DMF co-solvent can be applicable to charge reversal EHD co-jetting. Co-jetting with different solvent system for each needle is also possible as long as the polymer is not precipitated by the counter solvent. In addition, the fiber bundles of each polymer combination indicated the possibility of a continuous jetting process regardless of the type or combination of polymers, suggesting the superior jet stability of the reversal system compared to the forward system.

The bicompartamental architecture of the diverse polymer combinations was also analyzed using confocal Raman microscopy (**Figure 4**).<sup>[41]</sup> We first obtained characteristics Raman shifts of 4 single fibers jetted via charge reversal EHD co-jetting, comprising of TPU, PLGA, PMMA, and PVCi. Then, we mapped the bicompartamental microfibers based on the relative Raman intensity ratio of the distinguishable spectral region of each polymer as shown in right side of **Figure 4**. As shown in **Figure 4**, the two prominent colors of all mapping results indicated the successful formation of bicompartamental architecture regardless of polymer combination. In conjunction with CLSM images, these results provide solid evidence for the efficient applicability of the solution-based charge reversal EHD co-jetting method to prepare bicompartamental microfibers with diverse polymer combinations.

Furthermore, tricompartmental structures were also fabricated using charge reversal EHD co-jetting. Three needles were employed in parallel at the same height, each delivered with three different polymeric solutions, and jetted to fabricate triphasic microfibers.<sup>[42]</sup> Triphasic microfibers composed of TPU, PLGA, and PMMA are shown in **Figure 5**. As depicted in **Figure 5a**, a stable Taylor cone and continuous jet thread could be obtained, producing a well-defined fiber bundle. The CLSM image of the cross-section of the microfiber bundle (**Figure 5b**) showed three distinct colors corresponding to three compartments with well-preserved original needle architecture (inset of **Figure 5a**). The architecture was also clearly visible in the cross-sectional FE-SEM image (inset of **Figure 5b**). These results show that the proposed method can be extended to prepare multicompartmental microfibers with a tailored inner architecture.

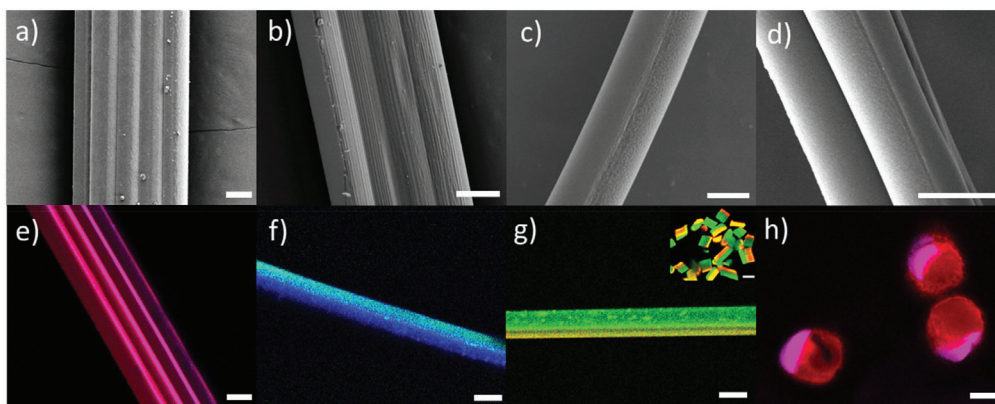


**Figure 3.** FE-SEM and CLSM images of biphasic microstructures in diverse polymer combinations. a,e) TPU and PMMA, b,f) PLGA and PVCi, c,g) PLGA and PMMA, d,h) PMMA and PVCi. The scale bar is 10  $\mu\text{m}$  in all images.

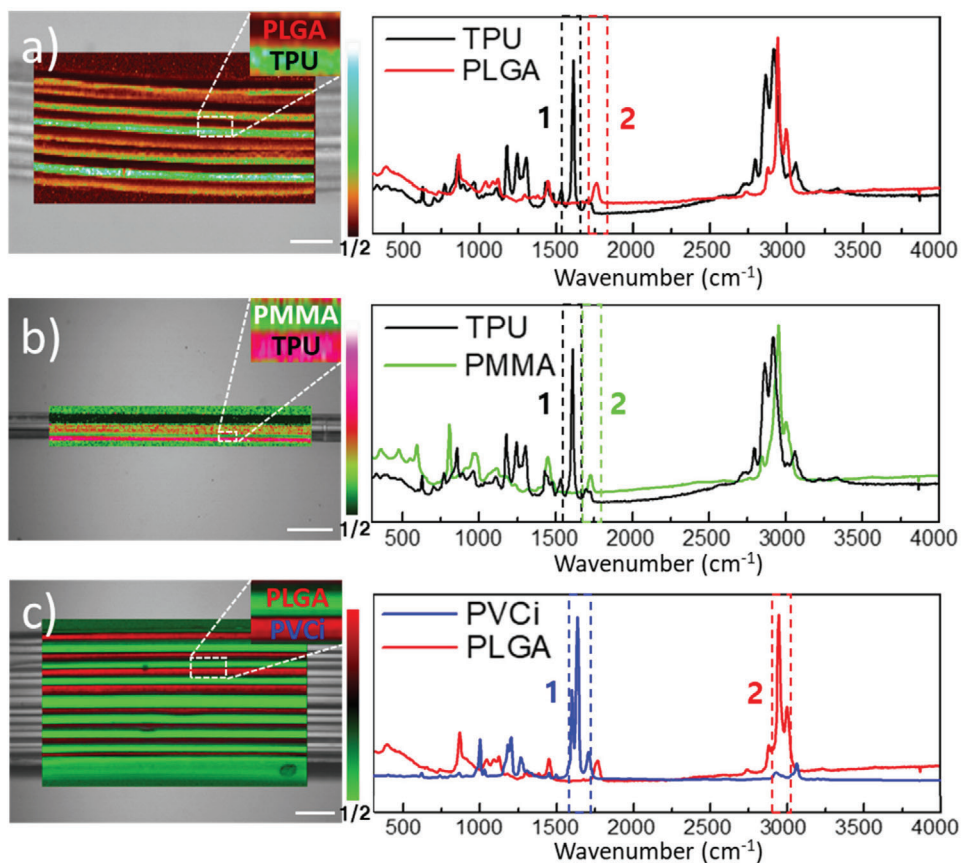


**Figure 4.** Confocal Raman mapping of biphasic microfibers in diverse polymer combinations with corresponding Raman spectra of a) TPU and PLGA, b) TPU and PMMA, and c) PVCi and PLGA. The scale bar is 50  $\mu\text{m}$  in all images.

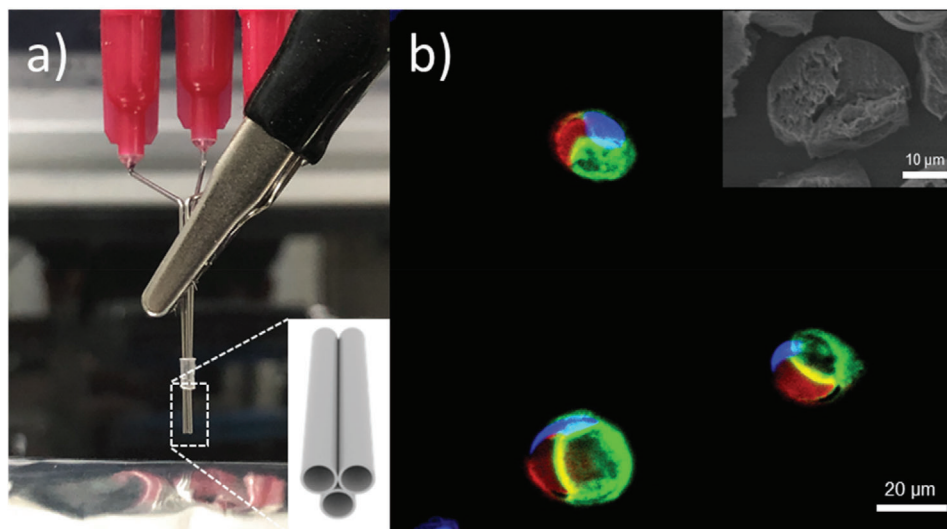


**Figure 5.** a) Digital photograph of triphasic EHD co-jetting via charge reversal (inset: needle configuration), and b) CLSM image of triphasic microcylinders with cross-sectional FE-SEM image (inset). TPU, PLGA, and PMMA are represented by blue, green, and red fluorescence dyes, respectively.

### 3. Conclusions

In summary, anisotropic compartmentalized microfibers composed of different polymeric materials were successfully fabricated via charge reversal EHD co-jetting. Combinations of various polymers such as TPU, PLGA, PMMA, and PVCi were utilized to fabricate multicompartmental microfibers. These fibers can be applied to a variety of fields based on their physical and chemical anisotropy. For example, a single TPU and PLGA-based biphasic microfiber could simultaneously exhibit different properties of each polymer in each compartment, such as flexibility of TPU and biodegradability of PLGA. Multicompartmental structures can also be fabricated by simply adjusting more needles and optimizing parameters such as applied voltage, flow rate, and polymer concentration.

### 4. Experimental Section

**Materials and Chemicals:** PMM ( $M_w = 120\,000\text{ g mol}^{-1}$ ), PLGA (85 : 15, ester terminated,  $M_w = 50\,000\text{--}75\,000\text{ g mol}^{-1}$ ), PVCi ( $M_w = 40\,000\text{ g mol}^{-1}$ ) were purchased from Sigma-Aldrich (USA). For fluorescent dye, poly[(m-phenylenevinylene)-co-(2,5-dioctoxy-p-phenylenevinylene)], fluorescein isothiocyanate isomer I, and rhodamine B isothiocyanate were also purchased from Sigma-Aldrich (USA) as blue, green, and red color, respectively. Tetrahydrofuran (THF; 99.8%), and N,N-dimethylformamide (DMF; 99.5%) were purchased from Samchun Chemical Co. Ltd. (Korea). TPU (Neothane) was purchased from Dongsung Co. Ltd. (Korea). All chemicals and materials were used as received without further purification.

**Preparation of Polymeric Microfibers and Microcylinders:** Polymeric solutions were prepared as 70% (w/v) of PLGA and PVCi, 20% (w/v) of TPU in THF/DMF (6:4, v/v), and 40% (w/v) PMMA in THF/DMF (5:5, v/v) for charge reversal EHD co-jetting. Fluorescent dyes contained a concentration of 0.01% (w/v). A dual capillary needle system consisting of side-by-side attached two fine gauge needles (25G, Nordson EFD, USA) was used to fabricate biphasic microfibers, whereas another needle was added for the triphasic microfibers. Two or three different polymeric solutions were jetted from the syringe pump at a flow rate of 150–200  $\mu\text{L h}^{-1}$ . High voltage (3.0–5.0 kV) was applied to the collector and the needle was connected to the ground electrode using a DC power supply (SHV50R, Conver-Tech Co., Korea). The needle tip-to-collector distance was set to  $\approx 5\text{--}10\text{ mm}$ . Microcylinders of length 20–50  $\mu\text{m}$  were prepared by cryo-sectioning of microfibers using a cryostat (CM 1850, Leica, Germany).

**Characterization:** FE-SEM (S-4800, Hitachi, Japan), CLSM (LSM 880 with Airyscan, ZEISS, Germany) were used to analyze the multicompartmental structure of the microfibers. For Raman 2D mapping, a RAMAN plus confocal laser Raman microscope (Nanophoton, Japan) with a 523 nm Nd:YAG laser source was used to analyze the multicompartmental structure of the microfibers. Raman spectra of each polymer were recorded in the range of 250–4000  $\text{cm}^{-1}$  with 1200  $\text{gr mm}^{-1}$  grating. The 2D Raman mapping images indicated the relative intensity ratio of area 1 and 2. The used spectral ranges of TPU/PLGA, TPU/PMMA, and PVCi/PLGA were 1606–1620/1753–1770, 1660–1620/1713–1739, and 1556–1673/2917–3031  $\text{cm}^{-1}$ , respectively.

### Acknowledgements

This research was supported by a National Research Foundation (NRF) grant (NRF-2020R1A4A2002590) and the Korea Evaluation Institute of Industrial Technology (KEIT) grant (20010853, 20013138).

### Conflict of Interest

The authors declare no conflict of interest.

### Data Availability Statement

The data that supports the findings of this study are available in the supplementary material of this article. All other data that support the findings of this study are available from the corresponding author upon reasonable request.

### Keywords

anisotropic compartmentalization, confocal Raman, electrohydrodynamics, electrospinning, Janus microfibers, polymer microfibers

Received: August 25, 2021

Revised: October 8, 2021

Published online: November 10, 2021

- [1] X. Dong, J. Zhang, L. Pang, J. Chen, M. Qi, S. You, N. Ren, *RSC Adv.* **2019**, *9*, 9838.
- [2] J. Lim, I. Jun, Y. B. Lee, E. M. Kim, D. Shin, H. Jeon, H. Park, H. Shin, *Macromol. Res.* **2016**, *24*, 562.
- [3] Z.-Q. Feng, K. Yan, J. Li, X. Xu, T. Yuan, T. Wang, J. Zheng, *Mater. Sci. Eng., C* **2019**, *104*, 110001.
- [4] D. F. Quevedo, N. Habibi, J. V. Gregory, Y. Hernandez, T. D. Brown, R. Miki, B. N. Plummer, S. Rahmani, J. E. Raymond, S. Mitragotri, J. Lahann, *Macromol. Rapid Commun.* **2020**, *41*, 2000425.
- [5] Q. Chen, S. C. Bae, S. Granick, *Nature* **2011**, *469*, 381.
- [6] E. Y. Hwang, J. S. Lee, D. W. Lim, *Langmuir* **2019**, *35*, 4589.
- [7] K. J. Lee, J. Yoon, J. Lahann, *Curr. Opin. Colloid Interface Sci.* **2011**, *16*, 195.
- [8] D. Suzuki, S. Tsuji, H. Kawaguchi, *J. Am. Chem. Soc.* **2007**, *129*, 8088.
- [9] B. Liu, W. Wei, X. Qu, Z. Yang, *Angew. Chem.* **2008**, *120*, 4037.
- [10] L. Liu, M. Ren, W. Yang, *Langmuir* **2009**, *25*, 11048.
- [11] T. Maric, M. Z. M. Nasir, R. D. Webster, M. Pumera, *Adv. Funct. Mater.* **2020**, *30*, 1908614.
- [12] J. Xu, D. H. C. Wong, J. D. Byrne, K. Chen, C. Bowerman, J. M. Desimone, *Angew. Chem., Int. Ed.* **2013**, *52*, 6580.
- [13] J. P. Rolland, B. W. Maynor, L. E. Euliss, A. E. Exner, G. M. Denison, J. M. Desimone, *J. Am. Chem. Soc.* **2005**, *127*, 10096.
- [14] H. Zhang, J. K. Nunes, S. E. A. Gratton, K. P. Herlihy, P. D. Pohlhaus, J. M. Desimone, *New J. Phys.* **2009**, *11*, 075018.
- [15] S. Xu, Z. Nie, M. Seo, P. Lewis, E. Kumacheva, H. A. Stone, P. Garstecki, D. B. Weibel, I. Gitlin, G. M. Whitesides, *Angew. Chem., Int. Ed.* **2005**, *44*, 724.
- [16] M. Xia, E. M. Go, K. H. Choi, J. H. Lim, B. Park, T. Yu, S. H. Im, S. K. Kwak, B. J. Park, *J. Ind. Eng. Chem.* **2018**, *64*, 328.
- [17] R. K. Shah, J.-W. Kim, D. A. Weitz, *Adv. Mater.* **2009**, *21*, 1949.
- [18] K. J. Lee, J. Yoon, S. Rahmani, S. Hwang, S. Bhaskar, S. Mitragotri, J. Lahann, *Proc. Natl. Acad. Sci. U. S. A.* **2012**, *109*, 16057.
- [19] W. Lv, K. J. Lee, J. Li, T.-H. Park, S. Hwang, A. J. Hart, F. Zhang, J. Lahann, *Small* **2012**, *8*, 3116.
- [20] M. Gil, S. Moon, J. Yoon, S. Rhamani, J.-W. Shin, K. J. Lee, J. Lahann, *Adv. Sci.* **2018**, *5*, 1800024.
- [21] S. Bhaskar, J. Lahann, *J. Am. Chem. Soc.* **2009**, *131*, 6650.
- [22] S. Hwang, K.-H. Roh, D. W. Lim, G. Wang, C. Uher, J. Lahann, *Phys. Chem. Chem. Phys.* **2010**, *12*, 11894.
- [23] W. Lv, K. J. Lee, S. Hwang, T.-H. Park, F. Zhang, J. Lahann, *Part. Part. Syst. Charact.* **2013**, *30*, 936.
- [24] T.-H. Park, K. J. Lee, S. Hwang, J. Yoon, C. Woell, J. Lahann, *Adv. Mater.* **2014**, *26*, 2883.
- [25] S. Bhaskar, J. Hitt, S.-W. L. Chang, J. Lahann, *Angew. Chem., Int. Ed.* **2009**, *48*, 4589.

- [26] J. Lee, T.-H. Park, K. J. Lee, J. Lahann, *Macromol. Rapid Commun.* **2016**, *37*, 73.
- [27] S. Bhaskar, K.-H. Roh, X. Jiang, G. L. Baker, J. Lahann, *Macromol. Rapid Commun.* **2008**, *29*, 1655.
- [28] K. J. Lee, S. Hwang, J. Yoon, S. Bhaskar, T.-H. Park, J. Lahann, *Macromol. Rapid Commun.* **2011**, *32*, 431.
- [29] K. J. Lee, T.-H. Park, S. Hwang, J. Yoon, J. Lahann, *Langmuir* **2013**, *29*, 6181.
- [30] A. Lee, H. Jin, H.-W. Dang, K.-H. Choi, K. H. Ahn, *Langmuir* **2013**, *29*, 13630.
- [31] H. Liu, S. Vijayavenkataraman, D. Wang, L. Jing, J. Sun, K. He, *Int. J. Bioprint.* **2017**, *3*, 009.
- [32] S. Moon, M. S. Jones, E. Seo, J. Lee, L. Lahann, J. H. Jordahl, K. J. Lee, J. Lahann, *Sci. Adv.* **2021**, *7*, eabf5289.
- [33] Y. Wang, L. Tian, T. Zhu, J. Mei, Z. Chen, D.-G. Yu, *Chem. Res. Chin. Univ.* **2021**, *37*, 443.
- [34] Z. Li, R. Liu, Y. Huang, J. Zhou, *J. Appl. Polym. Sci.* **2017**, *134*, 44687.
- [35] A. Kilic, F. Oruc, A. Demir, *Text. Res. J.* **2008**, *78*, 532.
- [36] U. Ali, X. Wang, T. Lin, *J. Text. Inst.* **2012**, *103*, 1160.
- [37] X. Zheng, S. Kang, K. Wang, Y. Yang, D.-G. Yu, F. Wan, G. R. Williams, S.-W. A. Bligh, *Int. J. Pharm.* **2021**, *596*, 120203.
- [38] Q. Tan, P. Irwin, Y. Cao, *IEEE Trans. Fundam. Mater.* **2006**, *126*, 1153.
- [39] R. R. Deshmukh, G. A. Arolkar, S. S. Parab, *Int. J. Chem. Phys. Sci.* **2012**, *1*, 40.
- [40] A. Cay, E. P. A. Kumbasar, C. Akduman, *Tekst. ve Konfeksiyon* **2015**, *25*, 38.
- [41] E. Sokolovskaya, J. Yoon, A. C. Misra, S. Bräse, J. Lahann, *Macromol. Rapid Commun.* **2013**, *34*, 1554.
- [42] S. Rahmani, S. Saha, H. Durmaz, A. Donini, A. C. Misra, J. Yoon, J. Lahann, *Angew. Chem., Int. Ed.* **2014**, *53*, 2332.